Numerical Simulation of the Effect of Gravity on Weld Pool Shape

A high gravitational field strongly affects the outward flow of the weld pool

BY J. DOMEY, D. K. AIDUN, G. AHMADI, L. L. REGEL AND W. R. WILCOX

ABSTRACT. Understanding the physical phenomena involved in the welding process is of substantial value to improving the weldability of materials. The intense heat and the arc inherent in fusion welding make direct experimental observation of the weld pool behavior rather difficult. Thus, numerical models that can predict the processes involved have become an invaluable tool for studying welding. One of the major factors affecting the motion within the molten weld pool is the gravity-driven buoyancy force. This force can act to oppose or enhance the Marangoni and/or electromagnetic driven convective flow within the weld pool. To study the effect of gravity on weld pool processes, a series of numerical simulations was performed. It was found that higher gravitational fields tend to enhance the convective flow within the weld pool and thus affect the heat transfer, the depth and width of the two phase region, and the pool depth-to-width ratio.

Introduction

According to David and DebRoy (Ref. 1), "Losses of life and property damage due to catastrophic failure of structures are often traced to defective welds." Since welding is such an important and widespread fabrication technique, it is imperative that a basic understanding of the physical processes involved become available. Until recently, welding has been thought of more as an art than a science with techniques developed through trial and error methods. Since welding is used in such a wide range of metal joining applications, from bicycles to nuclear reactor cores, providing a fundamental understanding of processes involved is of crucial interest to many fields. Several problems arise that cause defects within welds. One major source of defects is hot cracking. Factors affecting the hot-cracking susceptibility of an alloy fall into two categories: metallurgical and mechanical. The metallurgical factors are controlled by the composition and solidification morphology of the weldment. The mechanical factors are controlled by thermal stresses and strains. These mechanical factors occur in the material as it goes through its intense thermal cycle that causes the metal to solidify rapidly. Since these cracks are detrimental to the quality of the weldment, and ultimately the workpiece, it is beneficial to be able to develop a proper welding procedure so that hot cracking can be avoided. In order to achieve this goal, it is first necessary to understand the physical processes that occur during welding. The nature of arc welding does not allow direct observation during the welding process, and physical observation of the weld is limited to solidified welds. Thus, models which are capable of predicting the transient phenomena that are present during the welding process are needed to provide a better understanding of relationships between the microstructure and properties of welds (Ref. 1).

J. DOMEY, D. K. AIDUN and G. AHMADI are in the Mechanical and Aeronautical Engineering Department, and L. L. REGEL and W. R. WILCOX are in the International Center for Gravity Materials Science and Applications, Clarkson University, Potsdam, N.Y.

KEY WORDS

Numerical Simulation
Effect of Gravity
Weld Pool Shape
Weldability
Buoyancy Force
Fluid Flow
Convective Flow
Heat Transfer
GTAW
Aluminum Alloy 6061

Background

A brief review of the published literature on weld pool modeling is provided in this section. Most earlier models developed for the prediction of weld pool characteristics are limited by many simplifying assumptions. Some of the common restrictive assumptions that cause the models to be unrealistic include a prescribed weld pool profile, an undeformable weld pool surface, a stationary heat source, and a two-dimensional (2-D) simplification of a three-dimensional (3-D) problem. Only the model devel-

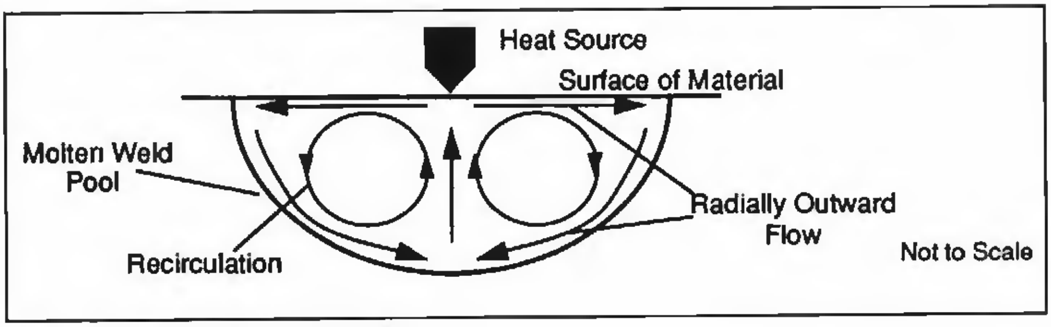

Fig. 1 — Schematic of buoyancy-driven flow.

oped by Zacharia, *et al.* (Ref. 2), relaxes many of these limitations and provides a realistic computational model for calculating weld pool characteristics.

In 1988, Zacharia, Eraslan, and Aidun (Refs. 2, 3) developed a 3-D transient model to simulate a moving gas tungsten arc (GTA) and a gas metal arc (GMA) welding process. The model incorporates a deformable surface and allows for mass addition and surface evaporation. The researchers found that the Marangoni forces were dominant, that surface deformation could retard Marangoni effects, and that the predicted surface deformation was in agreement with observation. Since the surface is completely deformable, the model accurately describes the phenomena of surface rippling and the weld "crown." In addition, the code may be applied to welding in microgravity conditions.

Paul and DebRoy (Ref. 4) used a 2-D model to simulate a low-power laser weld. Although their model assumed a rigid surface, they were able to superimpose the topography based on upward velocities at the surface with reasonable accuracy. Their results found fair agreement between numerical and experimentally determined surface topography, peak temperature, and secondary dendrite arm spacings.

Tsao and Wu (Ref. 5) presented a transient model that simulates both GMA and GTA welding processes. With their model they were able to account for the thermal energy addition of the filler metal within the arc. By applying this model to both GMA and GTA welding, they found that GMA penetrates three times faster than GTA under similar conditions. They also found that the surface properties have little influence on the GMA weld pool shape. The main influence on the increased weld penetration results from the molten filler metal (spray).

In 1989, Kaukler, *et al.* (Ref. 6), performed a conceptual study of laser beam welding in space. Their study consisted of performing laser beam melting and solidification experiments on board a NASA KC-135 airplane to indicate the most cost-effective technology for providing laser welding in space. Their experiments caused changes to heat transfer and morphology by varying the acceleration level alone. They concluded that acceleration-sensitive surface ripples were formed by surface tension gradients. They also noted that the optimal conditions for laser welding in space still need to be determined.

A 2-D transient model of the GTA weld process was formulated by Thompson and Szekely (Ref. 7). This model does not consider the effect of Lorenz forces, but does allow for the depression of the free surface. The model showed that the depression of the free surface can affect the maximum surface velocity by up to approximately 10%. It also can cause a change in the weld penetration approximately equal to the amount of the depression.

Tsotridis, Rother and Hondros (Ref. 8) constructed a 2-D transient model that simulates a laser weld process and was the first to account for heat losses due to surface evaporation. They found that Marangoni forces are dominant and that the weld profile near the surface is partially dependent upon the power of the laser beam.

Pardo and Weckman (Ref. 9) developed a 3-D finite element model for the calculation of steady-state temperatures in the GMA welding process. The model accounts for the release of the latent heat of fusion at the solid-liquid interface and is capable of predicting the weld reinforcement geometry. This model can also handle nonuniform velocity fields and surface geometries within the liquid weld pool.

Tsai and Kou (Ref. 10) developed a 2-D steady-state model to describe Marangoni convection within a weld pool. The pool surface as well as the liquid-solid boundary were calculated. The weld pool surface is calculated with the help of orthogonal curvilinear co-ordinates. They considered both a positive and negative surface tension temperature coefficient in their study. They found that when the surface tension gradient is negative the Marangoni flow is radially outward and the center of the pool surface is depressed while the outer portion of the pool is elevated. When the surface tension gradient is positive the reverse is true. They also found that pool depth can be significantly overestimated if the pool surface is assumed flat.

Recently, Zacharia and coworkers (Refs. 11, 12) used metallographic techniques to compare the actual fusion zone geometry of laser and GTA welds onto 304 stainless steel with their numerical simulation results. The model correctly predicts the shape of the fusion zones. They found that the weld bead is ob-

Table 1 — Thermophysical Properties and Weld Parameters

Property or Parameter	Value
Solidus temperature	582°C
Liquidus temperature	652°C
Vaporization temperature	2467°C
Reference density	2700 kg/m^3
Solidus density	2292 kg/m^3
Liquidus density	2241 kg/m^3
Magnetic permeability	1.26 (10^{-6}) H/m
Latent heat of fusion	1516 kJ/kg
Latent heat of vaporization	40,138 kJ/kg
Liquidus viscosity	0.375 (10^{-6}) m^2/s
Thermal conductivity of solid material	168 W/m•°C
Thermal conductivity of liquid material	108 W/m•°C
Specific heat, C_p	1.066 kJ/kg/K
Surface tension @ liquidus	9.14 (10^{-1}) kg/s^2
Surface tension gradient	−3.5 (10^{-7}) kg/s^2/°C
Arc current	150 A DCEN
Arc efficiency	100%
Arc power	3.153 kJ/s
Arc time	1.0 s
Room temperature	25.0°C
Effective radius of heat flux	0.003 m

tained as a result of the solidification of the liquid metal, so that the behavior of the liquid metal during solidification in the fusion zone should be considered an essential influence on the final properties of the weld.

In the present work, numerical simulations of GTA welds onto a material which has similar properties to that of the aluminum Alloy 6061 are presented for varying levels of gravity. The WELDER code is used for the theoretical prediction of the heat transfer processes involved in a standard GTA weld. The model considers the buoyancy, electromagnetic, and surface tension forces when solving for the overall heat transfer for a workpiece of finite size and shape. The model also accounts for phase change and considers the temperature dependence of the thermophysical properties. The relevant thermophysical properties for the material and the appropriate GTA welding process conditions are utilized in the simulation so that accurate results are obtained. The effects of gravity on the convection patterns and thermal conditions in stationary and moving weld pools are studied. The consequences of gravity on weld pool depth-to-width ratio is also discussed.

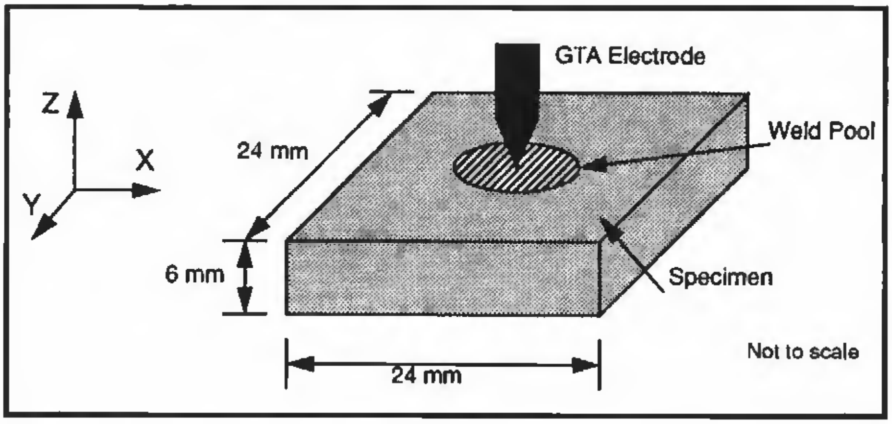

Fig. 2 — Schematic diagram of the workpiece and the weld pool.

Numerical Simulation

The WELDER code is a transient, three-dimensional computer simulation model which was developed for the investigation of coupled conduction and forced- and natural-convection heat transfer problems associated with the welding process. On the basis of modeling of physical phenomena, the special features of the code include: 1) realistic treatment of the molten surface of the weld pool as a deformable surface; 2) detailed consideration (without resorting to the Boussinesq approximation) of all of the densimetric-effect terms; 3) detailed consideration of the electromagnetic force effects; 4) accurate treatment of the mass addition to the weld pool (nonautogenous welding); 5) accurate treatment of the transient shape of the solid-liquid interface, according to a nonequilibrium (kinetic) phase-change model; 6) correct treatment of the combined surface-tension pressure and surface-tension-gradient effect (Marangoni shear-stress effect); 7) consideration of an arbitrary gravitational force (both low and high g); 8) consideration of the inclination of the workpiece relative to the gravitational force field (simulating out-of-position welding); 9) detailed consideration of surface cooling (convection and radiation); 10) realistic treatment of surface evaporation of the metal in the weld pool; and 11) accurate representation of the moving arc conditions (linear welds).

Special computational features include: 1) geometrically accurate composite-space-splitting discretization algorithm of the discrete-element-analysis; 2) composite-time-splitting explicit integration algorithm, with directional-transportive-upwind interpolation, which guarantees the stability of numerical solutions with second-order accuracy; and 3) marked-element formulation for accurate computation of the transient solid-liquid interface of the two-phase mushy-zone subregion.

The WELDER code is an explicit method and the time-steps are selected such that the 1) Courant-Friedrichs-Lewy criterion, 2) Courant criterion, and 3) Neumann criterion are satisfied. For a more complete description of the WELDER code, along with the discretization algorithm and all required stability criteria, one is referred to the work of Eraslan, *et al.* (Ref. 3).

Buoyancy-Driven Flow

The densimetric-coupling associated with the variation of the density of the liquid metal is included in the WELDER code. The local density of the liquid metal is considered as a constant reference value plus a generalized compressibility factor which represents the percent density variation with temperature (Ref. 2). That is:

$$\rho = \rho_o\left(1+\frac{\Delta\rho}{\rho_o}\right) = \rho_o(1+\beta) \quad (1a)$$

$$\beta = \beta(T) = \frac{\Delta\rho}{\rho_o}(T) \quad (1b)$$

where ρ is the local density, ρ_o is the reference density, β is the compressibility factor, and T is the temperature.

The gravitational force has a direct effect on the flow within a weld pool (through the buoyancy effect) and can be used to either enhance or deter the flow of molten material. When a fluid goes through a temperature change, there is also a corresponding change in its density. For welding, the incident heating upon the surface of the molten weld pool causes the melt to rise in temperature and, thus, go through a change in density. For most cases, the density decreases as the temperature increases.

A schematic of a buoyancy-driven flow pattern is shown in Fig. 1. This figure shows how the temperature gradient within a weld pool causes a corresponding density gradient and enhances the flow. When material of a higher temperature and lower density is forced to the bottom of a weld pool, the buoyancy force causes it to rise up through the center of the pool. The flow moves radially outward, the hot material is forced along the surface and then down the sides of the weld pool to the bottom. This leads to the circulation flow pattern shown in Fig. 1. The buoyancy-driven convection tends to decrease the depth-to-width ratio.

Earlier, the WELDER code was used by Domey, *et al.* (Ref. 13), to study welding process phenomena of a material with properties similar to that of the titanium alloy, Ti-6Al-4V. His results showed that the WELDER code is a suitable tool for the investigation of heat transfer phenomena involved in GTA welding.

Numerical Parameters

The simulations were performed for a stationary 150-A, direct current electrode negative (DCEN), 21-V GTA weld onto a 24 x 24 x 6-mm (1 x 1 x 1/4-in.) workpiece of a material with similar thermophysical properties to that of the aluminum Alloy 6061. This material was chosen due to its widespread use in the transportation industry. In order for a sim-

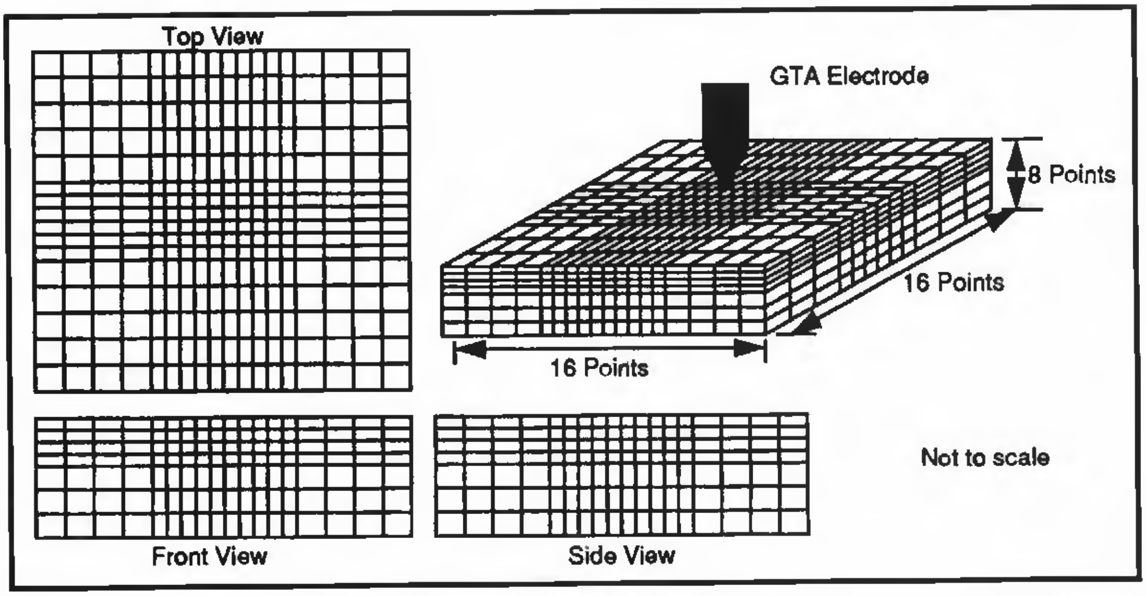

Fig. 3 — Grid system used in simulation.

ulation to predict accurate results, all of the relevant thermophysical properties for the given material must be known. The values for the thermophysical properties used in the present simulations are listed in Table 1.

As shown in Fig. 2, the workpiece is assumed to be completely surrounded by air at room temperature. This figure is a schematic diagram of the system that was used in both of the simulations. The electrode was placed directly over the center. Natural convection with the surroundings was assumed at the boundaries, with evaporation allowed from the liquid surfaces. For both of the stationary GTA weld simulations, the electrode was placed directly above the center of the surface of the specimen and held stationary throughout the simulation. The gravitational force was assumed to be acting normal to the surface of the workpiece and directed downward (the negative z direction).

The grid system employed in both the stationary and linear gas tungsten arc weld (GTAW) simulations was a 16 x 16 x 8 grid, as shown in Fig. 3. This figure shows the numerical grid system that was used in the simulations as the geometry was broken down into 16 divisions in each of the X and Y directions and 8 divisions in the Z direction. The divisions are smaller in the center and near the top where most of the "action" takes place. The spacings in the central area, where the weld pool forms, are smaller to improve resolution. Although this grid was relatively coarse, it provided results for quantitative analysis, while keeping the computational time within an acceptable limit. Should a finer mesh for a higher accuracy be desired, it could easily be implemented at the expense of additional computational time. A SPARC-station 2 GX, along with a 600 MB hard drive, was used to provide the necessary computational power and storage capability. The resulting data files from WELDER were plotted using Tecplot 5.0 and then printed using a PostScript laser printer.

Results

Several simulations were performed for different levels of gravity. The results of three of the transient simulations are shown in Fig. 4. Both the top views, as well as the side views, for the 0.1, 1.0 and 2.0-g simulations at a time of 1.0 s are shown. As can be seen from the figure, rather complex convection patterns are formed. The higher g produces greater velocities, as indicated by longer arrows. The Grashof number, which is the ratio of the buoyancy forces
to the viscous forces, is expressed as:

$$Gr = \frac{\beta g (T_s - T_\infty) L^3}{\upsilon^2} \qquad (2a)$$

where ß is the compressibility factor computed using Equation (1b) described earlier, T is temperature, L is length scale, and υ is the viscosity of the fluid. For the three cases presented here, the Grashof numbers have been computed and are: Gr(0.1 g) = 2.08 x 10^6, Gr(1.0 g) = 2.48 x 10^7, and Gr(2.0 g) = 1.56 x 10^8. In addition to the Grashof numbers, the Bond numbers have also been calculated. The Bond number, which is the ratio of the gravitational and surface tension forces, is expressed as:

$$Bo = \frac{\rho g L^2}{\sigma} \qquad (2b)$$

where L and σ are length scale and surface tension, respectively. The Bond numbers for the three cases are: Bo(0.1 g) = 0.190, Bo(1.0 g) = 2.04, and Bo(2.0 g) = 7.88.

At 0.1 g, the convection flow pattern is mostly due to a combination of the electromagnetic force (EMF) and the Marangoni force. This is because the buoyancy force is greatly reduced at this microgravity level. The roughly counterclockwise surface flow pattern observed for the 0.1-g case in Fig. 4 is oscillatory in nature. It is conjectured that this is due to the interaction between the EMF, Marangoni, surface tension, and buoyancy forces at this reduced gravity condition. Understanding the additional details of these phenomena requires further investigation and the results may be reported in a future paper.

For the 1.0-g case, the buoyancy-driven convection dominates the convection pattern and the flow is radially outward. The melt zone for the normal gravity condition is roughly similar in size to that of the 0.1-g case. At 2.0 g, however, the buoyancy-driven flow becomes very strong and results in relatively high convective velocity. That increases the heat flow rate, as well as the overall size of the weld pool.

The presented results show that for smaller g fields, the EMF and Marangoni forces dominate, whereas, buoyancy forces dominate at normal or high-gravity conditions. This is evident in comparing the Grashof numbers for the 0.1- and 2.0-g cases which are 2.08 x 106 and 1.56 x 108, respectively. The larger Grashof number in the 2.0-g case indicates that the buoyancy force has become more prominent in the higher g regime. The results also indicate that the buoyancy forces become more prominent than the surface-tension-related forces as the g-levels increase. This is in-

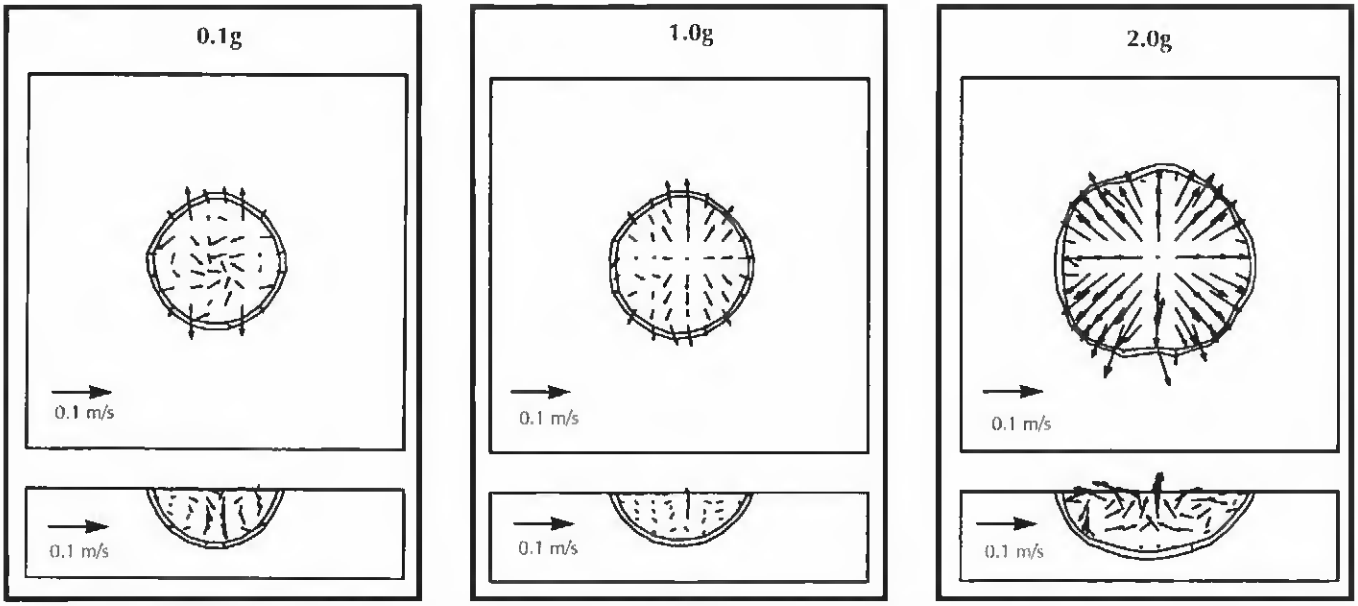

Fig. 4 — Stationary GTA welds at different gravity levels (g = earth's gravity).

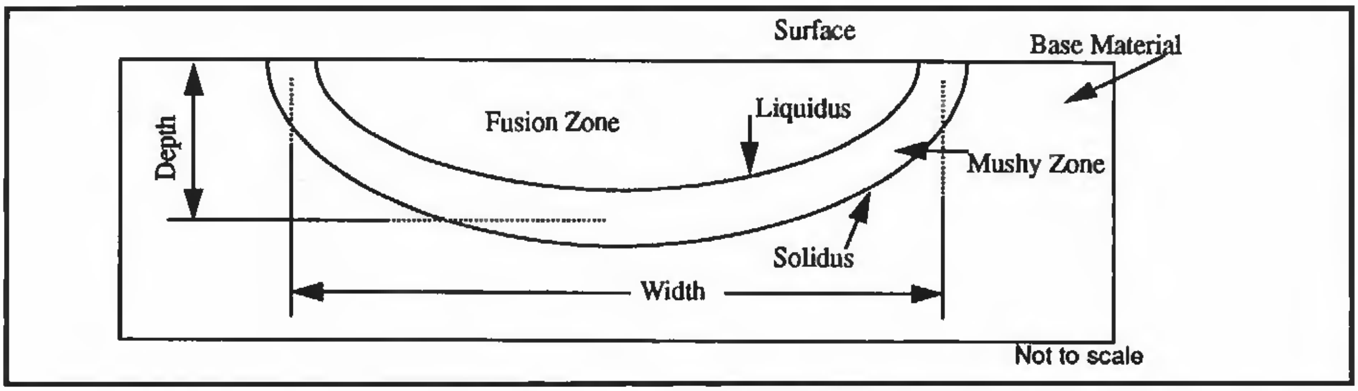

Fig. 5 — Definitions of depth, width and mushy zone.

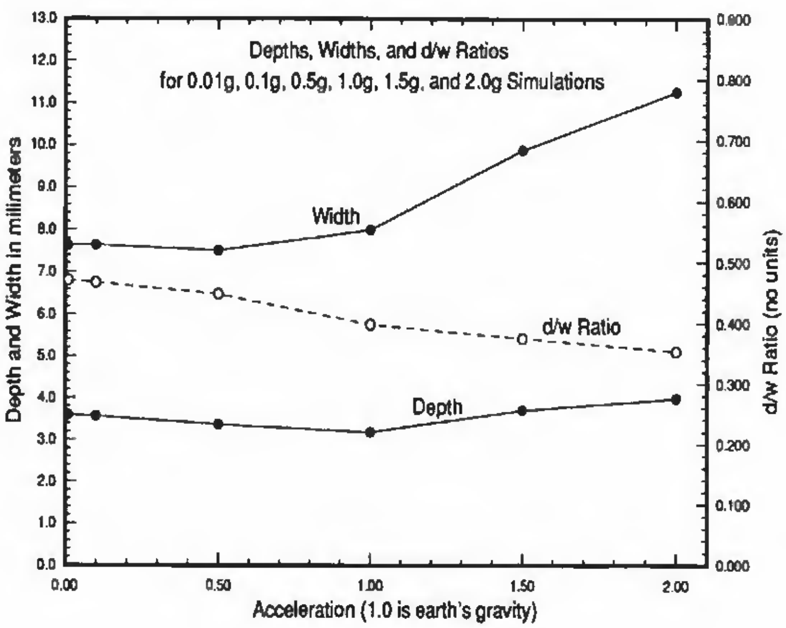

Fig. 6 — Depth, width and depth-to-width ratio vs. gravity level.

RESEARCH/DEVELOPMENT/RESEARCH/DEVELOPMENT/RESEARCH/DEVELOPMENT/RESEARCH/DEVELOPMENT

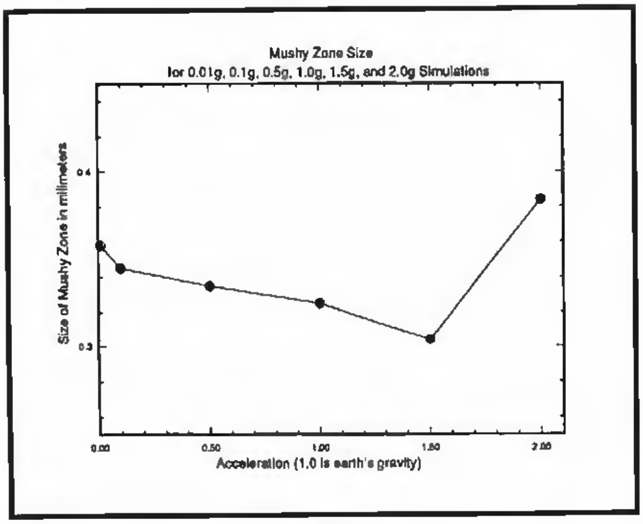

Fig. 7 — Mushy zone size vs. gravity level.

dicated by the Bond number for the 0.1-g case, Bo(0.1 g) = 0.190, which is much smaller than that for the 2.0-g case, Bo(2.0 g) = 7.88.

Weld Pool Shape and Mushy Zone

In this work, the depth of the weld pool was defined as the distance normal to the surface of the weld pool down to a point midway between the solidus and liquidus isotherms (Fig. 5). Similarly, the width was defined as the distance along the surface of the weld pool, as measured from the midway points between the solidus and liquidus isotherms across the diameter of the molten pool.

The depth, width, and depth-to-width ratio (d/w) are plotted vs. gravity in Fig. 6. As can be seen from the figure, high gravity causes both the depth and width of the weld to increase. The slope of the width line was greater than that of the depth line. This can also be seen by noting that the depth-to-width ratio has a slight negative slope, indicating that the gravitational effect on the heat transfer in the width direction was greater than in the depth direction.

The mushy zone, or two-phase region, was defined as the region bounded by the solidus and liquidus lines, as shown in Fig. 5. Although these isotherms are derived from the equilibrium phase diagram and a weld is a transient process, this definition allows for a quantitative comparison between simulations to be drawn. In Fig. 7, it can be seen that as the gravitational force was increased, the mushy zone size was slightly decreased until an acceleration of approximately 1.5 g. At this point the mushy zone size begins to increase indicating that the solidus isotherm was expanding into the base material faster than the liquidus isotherm. This phenomenon is currently under investigation.

Conclusions

Numerical simulations of a GTA welding process were performed for different levels of gravity. The results show that a high gravitational field causes an enhanced buoyancy-driven radially outward flow in the weld pool. This rather high-speed flow causes an increase in the heat transfer as compared to the lower gravity cases. The increased heat transfer affects the depth, width, d/w ratio and the size of the mushy zone. The depth and width both increase with an increase in the gravitational field, but the width grows more rapidly, resulting in a decreased d/w ratio. The mushy zone also increases slightly with a corresponding increase in the gravitational field. The results also show that at low-gravity conditions the electromagnetic driven convective flow becomes quite important.

Acknowledgments

This work was completed, in part, under the financial support of the National Aeronautics and Space Administration office of Life and Microgravity Science and Applications contract No. NGT-51345. The authors would also like to thank the reviewers for their helpful comments.

References

1. David, S. A., and DebRoy, T. 1992. *Science* 257:497.
2. Zacharia, T., Eraslan, A. H., and Aidun, D. K. 1988. *Welding Journal* 67:18-s.
3. Eraslan, A. H., Zacharia, T., and Aidun, D. K. 1986. Report No. MIE-142, Clarkson University, Potsdam, N.Y.
4. Paul, A. and DebRoy, T. 1988. *Metallurgical Transactions* B, Vol. 19B, pg. 851.
5. Tsao, K. C., and Wu, C. S. 1988. *Welding Journal*, 673:70-s.
6. Kaukler, W. F., Workman, G. L., and Plaster, T. 1989. *ASM Proceedings, Recent Trends in Welding Science and Technology*, p. 463.
7. Thompson, M. E., and Szekely, J. 1989. *International Journal of Heat and Mass Transfer*, 32:1007.
8. Tsotridis, G., Rother, H., and Hondros, E. D. 1989. *Naturwissensch* 76:216.
9. Pardo, E., and Weckman, D. C. 1989. *Metallurgical Transactions* B, 20B:937.
10. Tsai, M. C., and Kou, S. 1989, *International Journal for Numerical Methods in Fluids*, Vol. 9, p. 1503.
11. Zacharia, T., David, S. A., Vitek, J. M., and DebRoy, T. 1989. *Welding Journal* 68(12):499-s.
12. Zacharia, T., David, S. A., Vitek, J. M., and DebRoy, T. 1989. *Welding Journal*, 68(12):510-s.
13. Domey, J., Aidun, D. K., Ahmadi, G., and Diebold, T. 1992. *ASM Proceedings to the 3rd International Conference on Trends in Welding Research*, Gatlinburg, Tenn.